

# Coarse-grained dynamics of the freely cooling granular gas in one dimension

Mahendra Shinde,<sup>1,2,\*</sup> Dibyendu Das,<sup>3,†</sup> and R. Rajesh<sup>4,‡</sup>

<sup>1</sup>*Beijing National Laboratory for Condensed Matter Physics, Institute of Physics, Chinese Academy of Sciences, Beijing 100080, China*

<sup>2</sup>*Centre for Nonlinear Studies and the Beijing–Hong Kong–Singapore Joint Centre for Nonlinear and Complex Systems, Hong Kong Baptist University, Kowloon Tong, Hong Kong, China*

<sup>3</sup>*Department of Physics, Indian Institute of Technology Bombay, Powai, Mumbai 400 076, India*

<sup>4</sup>*Institute of Mathematical Sciences, Central Institutes of Technology Campus, Taramani, Chennai 600 113, India*

(Received 14 April 2011; published 29 September 2011)

We study the dynamics and structure of clusters in the inhomogeneous clustered regime of a freely cooling granular gas of point particles in one dimension. The coefficient of restitution is modeled as  $r_0 < 1$  or 1, depending on whether the relative speed is greater or smaller than a velocity scale  $\delta$ . The effective fragmentation rate of a cluster is shown to rise sharply beyond a  $\delta$ -dependent time scale. This crossover is coincident with the velocity fluctuations within a cluster becoming order  $\delta$ . Beyond this crossover time, the cluster-size distribution develops a nontrivial power-law distribution, whose scaling properties are related to those of the velocity fluctuations. We argue that these underlying features are responsible for the recently observed nontrivial coarsening behavior in the one-dimensional freely cooling granular gas.

DOI: [10.1103/PhysRevE.84.031310](https://doi.org/10.1103/PhysRevE.84.031310)

PACS number(s): 45.70.Mg, 45.70.Qj, 05.70.Ln

## I. INTRODUCTION

Consider a collection of particles, initially distributed randomly in space, evolving in time through ballistic transport and inelastic collisions. Such a system has been studied extensively as a simple model of granular systems as well as a tractable model in nonequilibrium statistical mechanics [1–13]. At initial times, the system undergoes homogeneous cooling, the energy decreasing with time  $t$  as  $t^{-2}$ , in accordance with Haff's law [14]. This law has been confirmed in experiments on particles under levitation [15] or in microgravity [16]. In this regime, the particles remain homogeneously distributed with interparticle spacing being the only relevant length scale.

Beyond a time scale  $t_c$ , this homogeneous cooling regime destabilizes [17] and the particles start clustering together, as has been confirmed through extensive simulations [3,6–13]. This regime is referred to as the inhomogeneous clustering regime. The energy decays as  $t^{-\theta}$ , where  $\theta$  varies with dimension and is different from 2 [1,6–10] in dimensions lower than the upper critical dimension, which is expected to be either infinity [1] or 4 [8]. In this regime, there is a growing length scale  $\mathcal{L}_t$ , determined by the size of the largest cluster.

Although direct experiments [15,16] do not probe the clustered regime as of now, there is the possibility of them doing so in the future. Furthermore, the effects of clustering are seen indirectly in experiments, for example, in the motion of granular gases following an impact [18], and can possibly be explained by studying simple models in lower dimensions [19]. The freely cooling granular gas problem is also important theoretically in its own right, as correlations are much more stronger than in driven systems: Conventional kinetic theory [17], which ignores strong correlations, describes driven

systems well, but is known to fail when compared to actual numerical simulations of the freely cooling system.

Much more is known in one dimension than in higher dimensions. Through an exact solution [4,5] of the problem with the coefficient of restitution set to zero (sticky gas) and extensive simulations [7] of the inelastic gas, it is known that  $\theta = 2/3$ . The sticky limit may also be mapped to the dynamics of shocks in the inviscid Burgers equation [20]. Recently, it was shown that when the coefficient of restitution depends on the impact velocity, a different time scale  $t_1$  further subdivides the inhomogeneous clustering regime into two subregimes [12,13]. This was based on a study of the density-density and velocity-velocity correlation functions. For times  $t_c < t < t_1$ , these structure functions scale exactly as in the sticky gas, obeying what is known as Porod's law [21]. However, for times  $t > t_1$ , the inelastic gas deviates from the sticky gas limit and the correlation functions violate Porod's law. In addition, the density distribution and interparticle distance distribution develop into power laws that are qualitatively different from that seen at earlier times. We will refer to the two subregimes as the Porod and fluctuation-dominated ordering regimes, respectively.

Although the macroscopic statistical quantities studied in Refs. [12,13] establish that the Porod and fluctuation-dominated ordering regimes are distinct, they do not reveal how fluctuations start dominating beyond the time scale  $t_1$ . It was speculated that the fluctuation-dominated ordering regime should have an effective process of fragmentation that will compete with the otherwise strong effective aggregation of clusters due to inelastic collisions. Whether coarse-grained density clusters break up or remain coherently moving objects can be checked directly by studying their dynamics. In this paper we study cluster dynamics, in particular effective fragmentation rates, and show that the ordering process gets disturbed beyond a certain time scale.

The second question is regarding the origin of the crossover time scale  $t_1$ . Earlier this was shown to depend on a velocity scale  $\delta$  associated with the coefficient of restitution [12,13].

\*mahendra.statp@gmail.com

†dibyendu@phy.iitb.ac.in

‡rajesh@imsc.res.in

The coefficient of restitution is often modeled as a function of the relative velocity, rather than being a constant, such that collisions become nearly elastic for relative velocities smaller than  $\delta$ . This property is consistent with experiments [22–24], required by theory [17], as well as essential in simulations to prevent inelastic collapse [2]. In this paper we demonstrate that the time  $t_1$  is marked by the particle velocity fluctuations within density clusters becoming of the order  $\delta$ . Thus it is not the typical velocities but rather the velocity fluctuations that matter for correlation functions. We also present a consistent scaling theory to explain the dependence of velocity fluctuations, fragmentation rates, and the cluster-size distribution on the parameters  $\delta$ , time  $t$ , and cluster size  $m$ .

In Sec. II we define the model and the quantities of interest and give details of the simulation. In Sec. III we present results from numerical simulations for velocity fluctuations, fragmentation rates, and the cluster-size distribution. We develop a scaling theory that enables us to understand the scaling of the above quantities in terms of two exponents. Section IV contains a summary and a discussion of results.

## II. MODEL AND DEFINITIONS

In this section we define the microscopic model and the quantities of interest. The model consists of a collection of  $N$  point particles of equal mass on a ring of length  $L$ . Each particle moves ballistically until it collides with another particle. The collisions conserve momentum but are inelastic such that when two particles with initial velocities  $u_i$  and  $u_j$  collide, the final velocities  $u'_i$  and  $u'_j$  are determined by

$$u'_{i,j} = u_{i,j} \left( \frac{1-r}{2} \right) + u_{j,i} \left( \frac{1+r}{2} \right), \quad (1)$$

where  $r$  is the coefficient of restitution. The particles are initially distributed randomly in space with their velocities drawn from a Gaussian distribution.

Experimentally, the coefficient of restitution depends on the relative velocity of the collision and is observed to tend to one (elastic) when the relative velocity tends to zero [22–24]. This is also true within viscoelastic theory [17] with  $r$  approaching 1 as  $(v/\delta)^\chi$ , with  $\chi = 1/5$  and  $\delta$  a velocity scale. However, experimentally,  $\chi$  is seen to take a range of values [22–24]. Theoretically,  $\delta$  has often been used as a tool merely to circumvent inelastic collapse in simulations. A simple model for  $r$  is often chosen, where  $\chi$  is chosen to be infinite [7,8]:

$$r(v_{\text{rel}}) = \begin{cases} r_0 & \text{if } v_{\text{rel}} > \delta, \\ 1 & \text{if } v_{\text{rel}} \leq \delta. \end{cases} \quad (2)$$

The collisions are elastic for relative velocities smaller than  $\delta$ . We adopt the same model for the coefficient of restitution. We stress that the existence of  $\delta$  is real and the phenomena arising due to a nonzero  $\delta$  should, in principle, be experimentally measurable provided one can go to large enough times. We have also simulated the system with  $r(v) = (1 - r_0) \exp[-(v/\delta)^\chi] + r_0$ , with  $\chi = 3.0$ . This choice of the coefficient of restitution smoothens the discontinuity present in Eq. (2). The results obtained for  $\chi = 3.0$  are consistent with the results obtained for  $r(v)$  with  $\chi = \infty$  as in Eq. (2). We thus expect that the results will not depend on the detailed

dependence of the coefficient of restitution on relative velocity as long as  $\chi > 1$ . When  $\chi < 1$ , it is no longer possible to avoid inelastic collapse in the event-driven simulations that we have done. However, conventional molecular-dynamics simulation with soft potentials suggest that the results also hold for  $\chi < 1$  [25].

Starting from the above microscopic model, we desire to study emergent processes such as fragmentation and aggregation of a collection of particles. To this end, a coarse-grained description has to be introduced, which we do as follows. Divide the ring into  $N$  equally sized boxes. Let the number of particles in the  $i$ th ( $i = 1, 2, \dots, N$ ) box be called the box density. We define a cluster as a collection of contiguous boxes with nonzero box density surrounded by two empty boxes. The total number of particles in this cluster will be called the size of the cluster. A similar definition has been used elsewhere; see, for example, Ref. [26]. In earlier papers [12,13] we studied velocity-velocity and density-density correlations using the coarse-grained box density. However, a single particle moving across the boundary of a box results in a change of density. To study clusters, any coarse graining should make sure that particles move significantly, i.e., by at least a box spacing  $L/N$ , to cause a change in configuration. The above definition of a cluster has this property.

The motion of particles within a cluster may be captured by studying the velocity fluctuations  $\sigma^2$ . Let  $\mathbf{u}_c$  be the center-of-mass velocity of a cluster, i.e.,  $\mathbf{u}_c = m^{-1} \sum_{i=1}^m \mathbf{u}_i$ , where  $\mathbf{u}_i$  are the velocities of the particles constituting the cluster and  $m$  is the size of the cluster. Then the velocity fluctuation of that cluster is  $\sigma^2(m, t) = m^{-1} \sum_{i=1}^m (\mathbf{u}_i - \mathbf{u}_c)^2$ , where the summation is again over all the particles constituting the cluster. When  $\sigma^2$  is much smaller than  $u_c^2$ , the cluster is compact and stable with respect to the velocity fluctuations. However, if they are of same order or if  $\sigma^2 \sim \delta^2$ , then the cluster may start breaking apart. This effect can be captured by defining an effective fragmentation rate of a cluster, as described below.

In the space of cluster sizes, a stochastic dynamics may be defined, with rates for the different processes being determined from simulations. As the clusters evolve in time due to the entry and exit of particles into and out of a cluster, we ask what the rates of transition from a cluster size  $m$  to  $m'$  are. Let  $W(m \rightarrow m'; t)$  be the rate at which a size  $m$  changes into a size  $m'$  at time  $t$ . If  $N(m, t)$  is the number of clusters per unit lattice site of size  $m$  at time  $t$ , then its time evolution is described by an effective master equation [27]

$$\frac{dN(m, t)}{dt} = \sum_{m'} W(m' \rightarrow m; t) N(m', t) - \sum_{m'} W(m \rightarrow m'; t) N(m, t). \quad (3)$$

If in a time interval  $\Delta t$ , the cluster size decreases, then the cluster is said to have undergone fragmentation. Thus an effective fragmentation rate  $W_f(m, t)$  of a cluster of size  $m$  at time  $t$  can be defined as

$$W_f(m, t) = \sum_{m' < m} W(m \rightarrow m'; t). \quad (4)$$

We note that, in Eq. (4), fragmentation is an emergent process, not defined *a priori* in the microscopic dynamics, unlike some other models of granular gas where fragmentation occurs on collision [28,29].

We study the model by means of event-driven molecular-dynamics simulations [30]. In the simulations the number density  $N/L$  is fixed to one and the number of particles  $N = 20\,000$ . The results in this paper do not depend on the precise values of the parameters  $r_0$  and  $\delta$ , as long as  $\delta$  is much smaller than the initial velocity differences of adjacent particles. We use generic values  $\delta = 0.001, 0.002, 0.004,$  and  $0.008$  and  $r_0 = 0.1$  in the simulations. The initial velocities are chosen from a Gaussian distribution with width 1. The data are typically averaged over 20 000–30 000 different initial conditions. All averages are over space and different histories and are denoted by  $\langle \cdot \cdot \rangle$ . Furthermore, we use reduced units in which all lengths are measured in terms of the initial mean interparticle spacing and times in terms of the initial mean collision time.

### III. RESULTS

In this section we study numerically three quantities: velocity fluctuations within a cluster, the effective fragmentation rate of a cluster, and the cluster-size distribution. We argue that their variation with time and cluster size can be captured by just two exponents. In addition, we also show the existence of a crossover time beyond which all three quantities show qualitatively different behavior and large compact clusters start breaking apart.

There are four velocity scales in the problem. First is the typical speed of a cluster that decreases in time as  $t^{-1/3}$  [4,7]. Second is the root-mean-square velocity fluctuations  $\sigma$  within a cluster (discussed in detail below). Third is  $\delta$ , characterizing the coefficient of restitution [see Eq. (2)], and the fourth corresponds to the initial velocity distribution. At large times, once the inhomogeneous cooling regime is reached, there is no memory of the initial velocity distribution, and it will play no role in the subsequent discussion. When the typical speeds become of order  $\delta$ , almost all collisions are elastic and energy no longer decreases. We will denote the latter crossover time by  $t_2$ . Clearly,  $t_2 \sim \delta^{-3}$ . It is possible that the velocity fluctuations scale with time differently from the typical velocity. If so, there is the possibility of a different crossover time, which is marked by the velocity fluctuations becoming order  $\delta$ . Beyond this crossover time, if it exists, intracluster collisions will be elastic while intercluster collisions continue to be inelastic and one might see a different structure at small scales.

We first characterize the velocity fluctuations  $\sigma^2$ . In Fig. 1 we show the variation of  $\sigma^2$  with time  $t$  for different values of  $\delta$  and two values of cluster size  $m$ . For short times,  $\sigma^2$  is independent of  $\delta$  and after initial transients it decays in time as a power law, with the exponent independent of  $m$  and the prefactor dependent on  $m$ . At large times,  $\sigma^2$  deviates from the power-law behavior and is constant before decreasing further. We argue that the flattening of the curve occurs when  $\sigma^2$  is of order  $\delta^2$ : Velocity fluctuations and hence relative velocities are such that most collisions within a cluster are elastic. Elastic collisions preserve the relative velocities before and after the

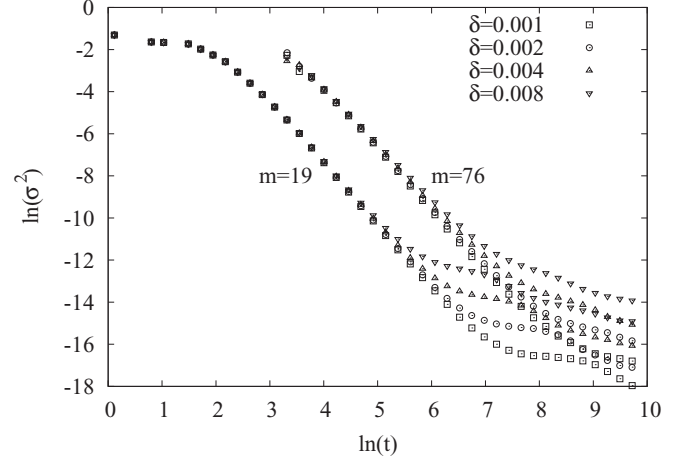


FIG. 1. Velocity fluctuations  $\sigma^2$  within a cluster of size  $m$  as a function of time  $t$  for different  $\delta$ . The data are for sizes  $m = 19$  and  $76$ . For short times the curves, for a given size, decay as a power law and are independent of  $\delta$ . Deviation from the power law is seen earlier for larger  $\delta$ .

collision and hence we expect  $\sigma^2$  to flatten out to a constant. These observations are mathematically summarized as

$$\sigma^2(t, \delta) \simeq \delta^2 f_1(t \delta^{2/x_1}) \quad \text{for fixed } m, \quad (5)$$

$$\sigma^2(t, m) \simeq f_2\left(\frac{t}{m^{x_2/x_1}}\right) \quad \text{for fixed } \delta, \quad (6)$$

where  $x_1$  and  $x_2$  are scaling exponents and  $f_1$  and  $f_2$  are scaling functions. Since the early time behavior of  $\sigma^2$  is independent of  $\delta$  (see Fig. 1),  $f_1(z) \sim z^{-x_1}$ ,  $z \ll 1$ . Similarly, consistency in the small- $t$  behavior between Eqs. (5) and (6) implies  $f_2(z) \sim z^{-x_1}$ ,  $z \ll 1$ . Thus, for fixed  $\delta$ ,  $\sigma^2 \sim m^{x_2} t^{-x_1}$  in the initial power-law phase.

The exponents  $x_1$  and  $x_2$  may be obtained from the data collapse in Fig. 1 when scaled as in Eqs. (5) and (6). The scaled data are shown in Figs. 2(a) [Eq. (5)] and 2(b) [Eq. (6)]. From these we obtain

$$x_1 = 3.00 \pm 0.06, \quad (7a)$$

$$x_2 = 2.66 \pm 0.08. \quad (7b)$$

Note that these values of  $x_1$  and  $x_2$  imply that the crossover time  $t_1$  relevant for  $\sigma^2$ , obtained by  $t_1 \delta^{2/x_1} \sim 1$ , implies that  $t_1 \sim \delta^{-2/x_1} \sim \delta^{-0.66}$ . This time scale is much smaller than  $t_2 \sim \delta^{-3}$ , which is the crossover time associated with the typical speed of particles becoming of order  $\delta$ , i.e., all collisions becoming nearly elastic. Therefore, we expect that the crossover time  $t_1$  should have no effect on the total energy of the system as long as  $t \ll t_2$ .

To confirm the independence of the total energy on  $t_1$  as well as to contrast the intracluster velocity fluctuations  $\sigma^2$  with typical cluster velocities, we study the center-of-mass velocity  $\mathbf{u}_c$  of a cluster. It is well known that the average energy per particle in the cooling gas decreases as  $t^{-2/3}$  [7]. Not surprisingly, we find that  $\langle u_c^2 \rangle$  for a cluster decays with the same law. In Fig. 3 we show the variation of  $\langle u_c^2 \rangle$  with time for different  $\delta$  and two different cluster sizes;  $\langle u_c^2 \rangle$  decreases as  $t^{-2/3}$  at large  $t$ . There is no signature of any crossover across

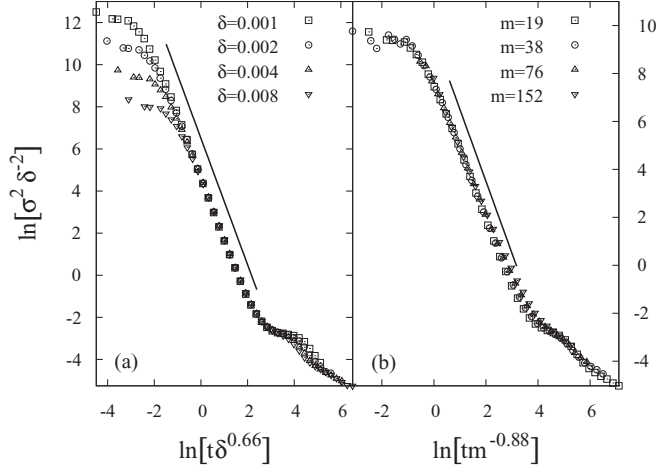


FIG. 2. Data collapse when scaled velocity fluctuations  $\sigma^2\delta^{-2}$  are plotted against (a) scaled time variable  $t\delta^{0.66}$  and (b) scaled time variable  $tm^{-0.88}$ . The data are for (a)  $m = 19$  and (b)  $\delta = 0.004$ . The solid straight lines have a slope of  $-3.0$ .

any intermediate time scale  $t_1$  nor any dependence on  $\delta$ . The intracluster collisions that are nearly elastic affect velocity fluctuations but not the typical speeds, which are affected only by cluster-cluster collisions.

We provide a further independent check for the numerical values of the exponents  $x_1$  and  $x_2$  in Eq. (7) by quantifying the velocity fluctuations  $\sigma_{\max}^2$  of the largest cluster in the system. From Eqs. (5) and (6) we obtain that  $\sigma_{\max}^2 \sim M_{\max}^{x_2} t^{-x_1}$ , where  $M_{\max}(t)$  is the size of the largest cluster at time  $t$ . Noting that  $M_{\max}(t) \sim t^{2/3}$  [4,7], we obtain  $\sigma_{\max}^2 \sim t^{2x_2/3-x_1} \sim t^{-1.22}$ , where we substituted the values of  $x_2$  and  $x_1$  from Eqs. (5) and (6). In Fig. 4 we show the variation of  $\sigma_{\max}^2$  with time  $t$  for different values of  $\delta$ . The temporal regime that is independent of  $\delta$  is consistent with the calculated value 1.22 of the exponent.

We now ask what the relevance of the crossover time  $t_1$  is. We show that though the typical speeds do not detect  $t_1$ , the

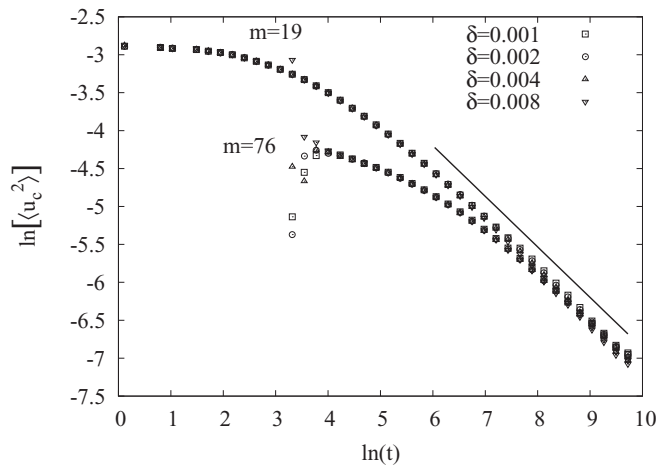


FIG. 3. Square of the center-of-mass velocity  $\langle u_c^2 \rangle$  of a cluster of size  $m$  as a function of time  $t$  for different  $\delta$ . The data are for sizes  $m = 19$  and  $76$ . For the times shown, there is no dependence on  $\delta$ , while for similar times the velocity fluctuations  $\sigma^2$  start depending on  $\delta$ . The solid line has a slope of  $-2/3$ .

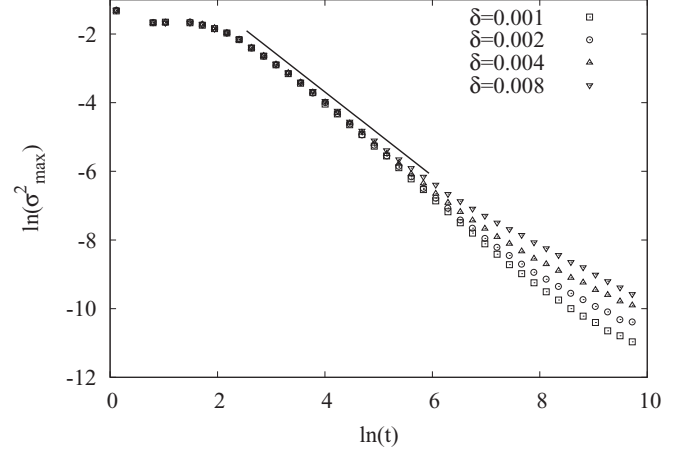


FIG. 4. Velocity fluctuations  $\sigma_{\max}^2$  of the largest cluster as a function of time  $t$  for different  $\delta$ . For short times the curves are independent of  $\delta$ . Deviation from the power law is seen earlier for larger  $\delta$ . The solid straight line has a slope of  $-1.22$ , as calculated from Eq. (7).

structure of the clusters changes drastically beyond  $t_1$ . Beyond  $t_1$ , intracluster collisions tend to be mostly elastic. Elastic collisions tend to smoothen out density inhomogeneities; therefore, clusters become less compact and we expect them to start fragmenting.

We show that the above crossover of  $\sigma^2$  from a power law is linked very closely to the initiation of fragmentation in clusters. The fragmentation rate  $W_f(m, t)$  as defined in Eq. (4) is measured numerically as follows. At time  $t$ , all the clusters of a particular size  $m$  are identified. At time  $t + \Delta t$ , the fraction of the identified clusters whose size has reduced is calculated. That fraction is equal to  $W_f(m, t)\Delta t$ . In the simulations, we choose  $\Delta t$  to be one so that sufficient statistics may be obtained.

In Fig. 5 we show the fragmentation rate  $W_f$  for cluster size 19 for different values of  $\delta$ . There is a sharp increase in the fragmentation rate beyond a certain time scale that is smaller for larger  $\delta$ . Thus the rise in the cluster fragmentation phenomenon understandably can be delayed by making the magnitude of the velocity scale  $\delta$  smaller, at which point elastic collisions dominate. In the inset of Fig. 5 we superimpose the fragmentation rate on the plot of  $\sigma^2$  with time for the same value of  $\delta$  and cluster size. Clearly, the time scale at which the fragmentation rate rises sharply coincides with  $t_1$ , the time scale beyond which the velocity fluctuations  $\sigma^2$  deviate from a power-law behavior. This increased fragmentation rate results in fluctuation-dominated coarsening and ultimately to the breakdown of Porod's law [12].

Another curious question is whether the larger masses are more stable to fragmentation than the smaller ones. To explore this, we studied the dependence of the fragmentation rate  $W_f$  on the cluster size. In Fig. 6 we show the variation of  $W_f$  with  $t$  for different  $m$  and fixed  $\delta$ . The crossover time beyond which increased fragmentation is seen increases with  $m$ . Having identified this crossover time with  $t_1$  (see the inset of Fig. 5), using Eq. (6) we write

$$W_f(t, m) \simeq m^\eta f_w \left( \frac{t}{m^{x_2/x_1}} \right) \quad \text{for fixed } \delta, \quad (8)$$

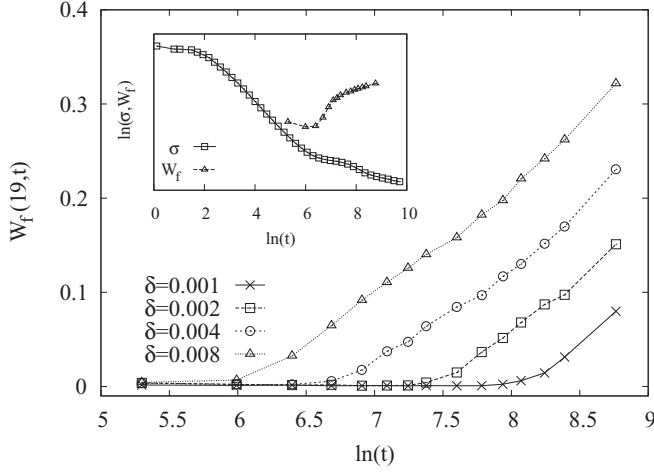


FIG. 5. Fragmentation rate  $W_f$  as a function of time  $t$  for different  $\delta$ .  $W_f$  shows a sharp increase beyond a time scale that is smaller for larger  $\delta$ . The data are for cluster size 19. Inset: Velocity fluctuations  $\sigma^2$  and  $W_f$  as a function of time. The increase in fragmentation rate coincides with saturation of the velocity fluctuations. The data are for  $\delta = 0.004$  and cluster size 19.

where  $\eta$  is an unknown exponent. We obtain excellent data collapse for  $\eta = 0.5$  [see the inset of Fig. 6].

From the dependence of fragmentation rate on mass size [Eq. (8)], we conclude that at a given time  $t$  (and given  $\delta$ ), masses up to a certain mass  $m^*(t, \delta)$  undergo fragmentation. We believe that this is the origin of the breakdown of Porod's law, as fragmentation results in new structures at small scales. One way to capture this is to study the average cluster-size distribution  $\langle N(m, t) \rangle$ , where  $N(m, t)$  is the number of clusters of size  $m$  at time  $t$  and the average is over space and histories. We would like to investigate whether, in the presence of fragmentation, the cluster-size distribution can be explained by knowing the cluster-size distribution of the sticky gas (zero coefficient of restitution). We argue below that while some regimes of  $\langle N(m, t) \rangle$  resemble the sticky gas, other regimes

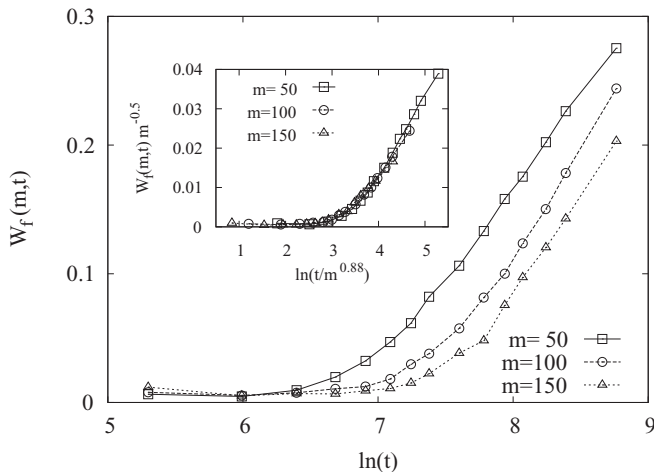


FIG. 6. Fragmentation rate  $W_f$  as a function of time  $t$  for different cluster sizes  $m$ . Larger clusters are more stable and start fragmenting at a later time. The data are for  $\delta = 0.008$ . Inset: Data collapse when  $W_f$  and time are scaled as in Eq. (8) with  $\eta = 0.5$ .

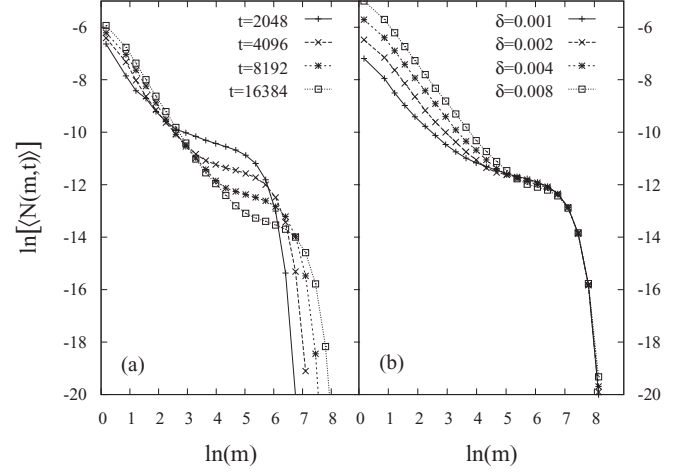


FIG. 7. Average cluster distribution  $\langle N(m, t) \rangle$  as a function of cluster size  $m$  for (a) fixed  $\delta = 0.004$  and different times and (b) different  $\delta$  and fixed time  $t = 16384$ . While the small mass behavior of  $\langle N(m, t) \rangle$  depends on  $\delta$ , the large mass behavior of  $\langle N(m, t) \rangle$  is independent of  $\delta$ .

differ, but their scaling may be obtained from that of  $\sigma^2(m, t)$ , following Eqs. (5)–(7).

The mean cluster-size distributions are shown for different times in Fig. 7(a) and for different  $\delta$  in Fig. 7(b). We note that for fixed time,  $\langle N(m, t) \rangle$  for large masses has no dependence on  $\delta$  [see Fig. 7(b)]. Thus we expect that for masses greater than a mass cutoff  $m^*(t, \delta)$ , fragmentation is not relevant. Therefore, for masses larger than  $m^*(t, \delta)$ ,  $\langle N(m, t) \rangle$  should have the same scaling behavior as in the sticky gas. For the sticky gas, it is known [4] that

$$\langle N(m, t) \rangle \simeq \frac{1}{t^{4/3}} f_3\left(\frac{m}{t^{2/3}}\right), \quad (9)$$

where the scaling function  $f_3(z) \sim z^{-1/2}$  for  $z \ll 1$  and  $f_3(z) \rightarrow 0$  for  $z \gg 1$ . For masses  $m > m^*(t, \delta)$  for which fragmentation is not important, we confirm numerically that the same scaling holds. In Fig. 8 we scale the data of Fig. 7(a) as in Eq. (9) and we see excellent data collapse for large cluster sizes, confirming that fragmentation can be neglected for cluster sizes larger than  $m^*(t, \delta)$ .

We note that in Fig. 8 there is no data collapse for small cluster sizes when the data is scaled as in Eq. (9), showing that when fragmentation is relevant, the cluster-size distribution gets modified. We argue that the small mass scaling can be obtained by knowing the scaling of  $\sigma^2$ . For a fixed  $\delta$  and varying  $t$ ,  $\langle N(m, t) \rangle$  should have the scaling form [using Eq. (6)]

$$\langle N(m, t) \rangle \simeq \frac{1}{t^\alpha} f_4\left(\frac{m}{t^{x_1/x_2}}\right), \quad m \ll m^* \text{ for fixed } \delta, \quad (10)$$

where  $\alpha$  is an exponent that we determine by examining the large- $z$  behavior of the scaling function  $f_4(z)$  and  $x_1$  and  $x_2$  are as in Eq. (7). For large  $z$ ,  $f_4(z)$  should be such that it crosses over to the small- $z$  behavior of  $f_3(z)$ . Thus  $f_4(z) \sim z^{-1/2}$  for

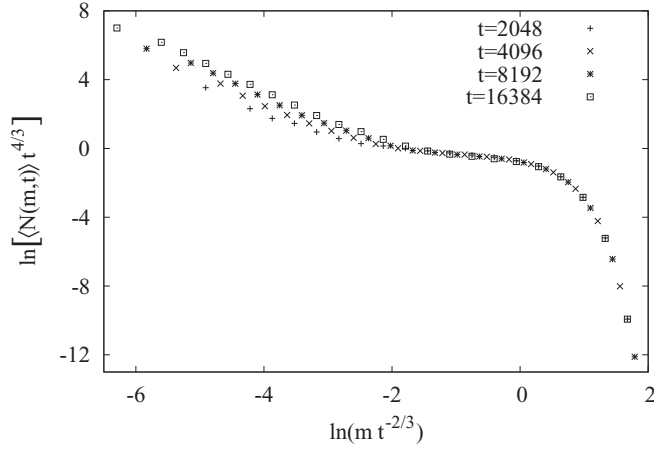


FIG. 8. Data collapse for large cluster sizes  $m$  when the cluster distribution  $\langle N(m,t) \rangle$  and  $m$  are scaled as in Eq. (9), a scaling form identical to that obeyed by  $\langle N(m,t) \rangle$  in the sticky gas. The data collapse shows that fragmentation is irrelevant for masses beyond a critical mass  $m^*(t, \delta)$ . The data at small masses do not collapse, showing that when fragmentation is relevant, the scaling is modified. The data are for  $\delta = 0.004$ .

$z \gg 1$ . Comparing the time dependence of Eqs. (9) and (10) in the latter limit, we obtain

$$\alpha = 1 + \frac{x_1}{2x_2} \approx 1.56. \quad (11)$$

The data, when scaled as in Eqs. (10) and (11) with  $x_1$  and  $x_2$  as in Eq. (7), are shown in Fig. 9(a). We obtain good data collapse for the small cluster sizes (while the large masses no longer collapse), showing that knowledge of the scaling behavior of  $\sigma^2$  is sufficient to obtain the scaling behavior of  $\langle N(m,t) \rangle$ . The small- $z$  behavior of  $f_4(z)$  can be determined numerically. We find that  $f_4(z) \sim z^{-\tau}$  with  $\tau = 1.75 \pm 0.08$  [see the solid line in Fig. 8(a)].

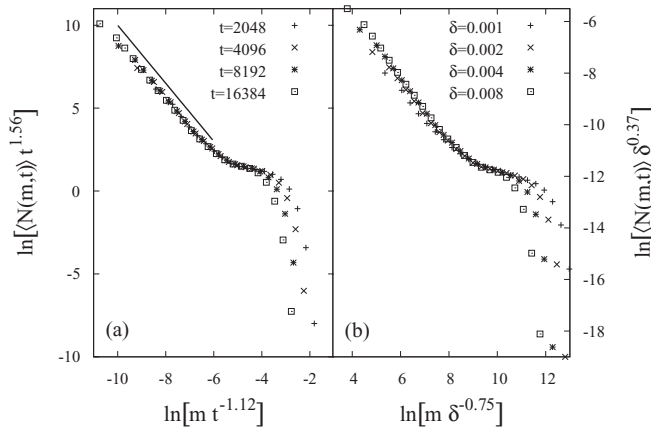


FIG. 9. Data collapse for small cluster sizes  $m$  when the cluster distribution  $\langle N(m,t) \rangle$  and  $m$  are scaled as in (a) Eq. (10) for fixed  $\delta = 0.004$  and (b) Eq. (12) for fixed  $t = 16384$ . The solid line has a slope of 1.75. Note that the data for large masses no longer collapse.

The scaling of the small cluster sizes with  $\delta$  can also be obtained from the scaling of  $\sigma^2$ . Knowing that  $m^*$  scales as  $\delta^{2/x_2}$  and using Eqs. (5) and (6), we write

$$\langle N(m, \delta) \rangle \simeq \frac{1}{\delta^\beta} f_5\left(\frac{m}{\delta^{2/x_2}}\right), \quad m \ll m^* \text{ for fixed } t, \quad (12)$$

where the exponent  $\beta$  can be determined by constraining the large- $z$  behavior of the scaling function  $f_5(z)$  to be the same as the small- $z$  behavior of  $f_3(z)$ . This immediately implies that  $f_5(z) \sim z^{-1/2}$  for  $z \gg 1$  and

$$\beta = \frac{1}{x_2} \approx 0.37. \quad (13)$$

The data for the cluster-size distribution, when scaled as in Eqs. (12) and (13) with  $x_1$  and  $x_2$  as in Eq. (7), are shown in Fig. 9(b). We obtain reasonable data collapse for the small cluster sizes. However, given the range and quality of data, it is possible to obtain data collapse for a range of  $x_2$ .

We thus demonstrated that the scaling of the cluster-size distribution  $\langle N(m,t) \rangle$  with time and  $\delta$  can be obtained by knowing the scaling of  $\sigma^2$ . We also showed that beyond the crossover time  $t_1$ , the cluster distribution has a richer structure than that of the sticky gas. In Refs. [12,13] we showed that modification of  $\langle N(m,t) \rangle$  results in the two-point density-density and velocity-velocity correlation functions violating Porod's law. Thus we conclude that the increased fragmentation rate brought about by velocity fluctuations becoming of order  $\delta$  is most probably the reason behind the violation of Porod's law.

#### IV. DISCUSSION

To summarize, we studied velocity fluctuations, effective fragmentation rates, and the size distribution of clusters in a freely cooling granular gas on a one-dimensional ring, evolving via ballistic motion and inelastic collisions. The coefficient of restitution was  $r_0 < 1$  for relative velocity greater than  $\delta$  and 1 otherwise. The aim of the paper was to understand the consequences of a nonzero  $\delta$  on the structure of clusters at large times.

This study was motivated by the recent finding that for granular gases with a realistic velocity-dependent coefficient of restitution, the nature of coarsening in the inhomogeneous cooling regime is not the same at all times [12,13]. Beyond a crossover time scale  $t_1$ , the coarsening behavior changes at the macroscopic level from one that obeys Porod's law to one that violates Porod's law. These interesting numerical findings lacked an explanation on a mesoscopic scale of how and why the crossover occurs. The present paper provides an explanation. We demonstrate in this paper that the transition from the sticky gas regime, where Porod's law is obeyed, to a fluctuation-dominated ordering regime, where Porod's law is violated, all within the inhomogeneous cooling regime, may be viewed as a growing dominance of an underlying fragmentation process competing against the clustering process. The fact that clusters break up is shown by the quantitative change in the behavior of the velocity fluctuations within a cluster. This crossover in velocity fluctuations coincides with an increase in the fragmentation rate of clusters leading to a richer fine structure reflected in the density-density correlations.

More specifically, the velocity fluctuations within a cluster were found to decrease in time as a power law with time, with the velocity fluctuations being much smaller than the center of mass velocities. However, when these fluctuations became of order  $\delta$ , nearly all intracluster collisions were elastic and the clusters started to fragment. The crossover was captured in terms of two exponents  $x_1$  and  $x_2$ . This emergent phenomenon was further quantified by defining an effective fragmentation rate for a cluster. The fragmentation rate was seen to rise sharply at a cluster-size-dependent time with the crossover time increasing with decreasing  $\delta$ . The crossover time was shown to be the same as that seen in the velocity fluctuations. Once fragmentation set in, the cluster-size distribution  $\langle N(m,t) \rangle$  changed drastically from that of the sticky gas ( $r_0 = 0$ ,  $\delta = 0$ ). However, the scaling of  $\langle N(m,t) \rangle$  could be captured by the same exponents  $x_1$  and  $x_2$  used to describe the velocity fluctuations  $\sigma^2(m,t)$ . It was also observed that the total energy of the system and clusters continue to decay as  $t^{-2/3}$ , showing no signature of the structural changes in the clusters.

We believe that many of these (qualitative) results will be carried over to higher dimensions. In two dimensions, for coarse-grained velocities it was shown [8] that the velocity fluctuations scale differently from the typical velocity. Hence we expect a crossover when these fluctuations become comparable to  $\delta$  and thus fragmentation to be relevant for two dimensions too and, consequently, a regime where coarsening is fluctuation dominated. Earlier studies show that density-density and velocity-velocity correlations obey Porod's law in two dimensions [11]. However, these studies were done at interme-

diated densities and short times. It would be interesting to verify whether a fluctuation-dominated regime exists at large times.

The velocity scale  $\delta$  is relevant experimentally and not just a computational tool. Experimentally,  $r(v)$  approaches 1 when the relative velocity  $v$  tends to zero, i.e.,  $1 - r(v) = g(v/\delta)$ , where  $g(x) \sim x^\chi + O(x^{2\chi})$  for  $x \ll 1$  and  $g(x) \sim O(1)$  for  $x \rightarrow \infty$ . Experimentally, the exponent  $\chi$  takes a variety of values. Within the framework of viscoelastic theory,  $\chi = 1/5$ . Systems with  $\chi < 1$  cannot be studied using event-driven molecular-dynamics simulations (as in the present paper) as inelastic collapse prevents the simulation from proceeding forward. Results from preliminary molecular-dynamics simulations with soft potentials suggest that the results in this paper continue to hold for  $\chi < 1$ .

Another question of interest is the construction of lattice models that reproduce the coarse-grained behavior of the granular gas. Such models not only are computationally much faster, but also may be the first steps toward building effective field theories for the system. In a recent paper [31] a stochastic lattice model was studied that reproduced all features of the sticky gas. It would be interesting to see whether fragmentation can be incorporated into this lattice model such that the coarse-grained behavior seen in the present paper is reproduced.

#### ACKNOWLEDGMENTS

M.S. was partially supported by the Institute of Physics, Chinese Academy of Sciences under the Grant No. 2011001. Part of this work (M.S.) was carried out at the Centre for Nonlinear Studies, Hong Kong Baptist University.

- 
- [1] G. F. Carnevale, Y. Pomeau, and W. R. Young, *Phys. Rev. Lett.* **64**, 2913 (1990).
  - [2] S. McNamara and W. R. Young, *Phys. Fluids A* **4**, 496 (1992).
  - [3] I. Goldhirsch and G. Zanetti, *Phys. Rev. Lett.* **70**, 1619 (1993).
  - [4] L. Frachebourg, *Phys. Rev. Lett.* **82**, 1502 (1999).
  - [5] L. Frachebourg, P. A. Martin, and J. Piasecki, *Physica A* **279**, 69 (2000).
  - [6] S. Chen, Y. Deng, X. Nie, and Y. Tu, *Phys. Lett. A* **269**, 218 (2000).
  - [7] E. Ben-Naim, S. Y. Chen, G. D. Doolen, and S. Redner, *Phys. Rev. Lett.* **83**, 4069 (1999).
  - [8] X. Nie, E. Ben-Naim, and S. Chen, *Phys. Rev. Lett.* **89**, 204301 (2002).
  - [9] E. Trizac and A. Barrat, *Eur. Phys. J. E* **3**, 291 (2000).
  - [10] E. Trizac and P. L. Krapivsky, *Phys. Rev. Lett.* **91**, 218302 (2003).
  - [11] S. Das and S. Puri, *Phys. Rev. E* **68**, 011302 (2003).
  - [12] M. Shinde, D. Das, and R. Rajesh, *Phys. Rev. Lett.* **99**, 234505 (2007).
  - [13] M. Shinde, D. Das, and R. Rajesh, *Phys. Rev. E* **79**, 021303 (2009).
  - [14] P. Haff, *J. Fluid Mech.* **134**, 401 (1983).
  - [15] C. C. Maaß, N. Isert, G. Maret, and C. Aegerter, *Phys. Rev. Lett.* **100**, 248001 (2008).
  - [16] S. Tatsumi, Y. Murayama, H. Hayakawa, and M. Sano, *J. Fluid Mech.* **641**, 521 (2009).
  - [17] N. V. Brilliantov and T. Pöschel, *Kinetic Theory of Granular Gases* (Oxford University Press, Oxford, 2004).
  - [18] J. F. Boudet, J. Cassagne, and H. Kellay, *Phys. Rev. Lett.* **103**, 224501 (2009).
  - [19] Z. Jabeen, R. Rajesh, and P. Ray, *Euro. Phys. Lett.* **89**, 34001 (2010).
  - [20] S. Kida, *J. Fluid Mech.* **93**, 337 (1979).
  - [21] G. Porod, *Small-Angle X-Ray Scattering* (Academic, London, 1982).
  - [22] C. V. Raman, *Phys. Rev.* **12**, 442 (1918).
  - [23] L. Labous, A. D. Rosato, and R. N. Dave, *Phys. Rev. E* **56**, 5717 (1997).
  - [24] E. Falcon, C. Laroche, S. Fauve, and C. Coste, *Euro. Phys. J. B* **3**, 45 (1998).
  - [25] S. N. Pathak, D. Das, and R. Rajesh (unpublished).
  - [26] C. Huepe and M. Aldana, *Phys. Rev. Lett.* **92**, 168701 (2004).
  - [27] N. G. V. Kampen, *Stochastic Processes in Physics and Chemistry* (Elsevier, Amsterdam, 2007).
  - [28] I. Pagonabarraga and E. Trizac, in *Granular Gas Dynamics*, edited by T. Pöschel and N. Brilliantov, Lecture Notes in Physics, Vol. 624 (Springer-Verlag, Berlin, 2003), p. 163.
  - [29] R. C. Hidalgo and I. Pagonabarraga, *Europhys. Lett.* **77**, 64001 (2007).
  - [30] D. C. Rapaport, *The Art of Molecular Dynamics Simulations* (Cambridge University Press, Cambridge, 2004).
  - [31] S. Dey, D. Das, and R. Rajesh, *Euro. Phys. Lett.* **93**, 44001 (2011).